IEEE Access
Multidisciplinary | Rapid Review | Open Access Journal

Received February 1, 2019, accepted March 7, 2019, date of publication March 21, 2019, date of current version April 8, 2019.

Digital Object Identifier 10.1109/ACCESS.2019.2905514

Object Tracking Over Distributed WSNs With Consensus on Estimates and Missing Data

MIGUEL VAZQUEZ-OLGUIN, (Member, IEEE), YURIY S. SHMALIY, (Fellow, IEEE), OSCAR IBARRA-MANZANO, (Member, IEEE), JORGE MUNOZ-MINJARES, (Member, IEEE), AND CARLOS LASTRE-DOMINGUEZ, (Member, IEEE)
Department of Electronics Engineering, Universidad de Guanajuato, Salamanca 36885, Mexico
Corresponding author: Yuriy S. Shmaliy (shmaliy@ugto.mx)

ABSTRACT Wireless sensor network (WSN) technologies are used to provide mobile object tracking due to advantages such as mobility, scalability, and flexibility. However, wireless interaction between the network nodes is often accompanied by missing data, which requires robustness from the estimator. This paper develops an iterative distributed unbiased finite impulse response (dUFIR) filtering algorithm for object tracking via WSNs with consensus on estimates and shows that it has higher robustness than the distributed Kalman filter (dKF). The tracking problem is viewed as a real-time position estimation of an unmanned ground vehicle (UGV). The extensive simulations are provided using real sensor parameters and measurements of the UGV position with missing data. Two different scenarios are considered when: 1) each sensor is capable of measuring the UGV position and 2) sensors have different time-varying noise variances, as in practical WSNs. The higher robustness of the dUFIR against the dKF is demonstrated under diverse operation conditions.

INDEX TERMS Distributed wireless sensor network, object tracking, unbiased FIR filter, Kalman filter, robustness, consensus on estimates.

I. INTRODUCTION

Target tracking of moving objects is an application that benefits from unique advantages of wireless sensor networks (WSNs) [1]–[3] such as a massive nodes deployment, capacity of distributed processing, and ubiquitous integration with the environment. An example of indoor target tracking is shown in Fig. 1, where a WSN covers the moving object trajectory. A specific is that, due to the WSN restrictions, algorithms capable of estimating the position of a mobile object must comply with a sufficient accuracy and robustness required to provide tracking in the presence of model errors, missing data, and not completely known noise statistics. Therefore, optimal estimators and fusion techniques taking advantages of redundant and distributed measurements are often used to provide best noise reduction for WSN structures [4]–[11].

For target tracking, the WSNs can be organized to have either a centralized, decentralized, or distributed structure [5]. The latter is known to be most powerful, flexible, and energy efficient [12]–[14]. Furthermore, it may provide even better estimates if to take advantage of different kinds of consensuses such as on measurements [15], estimates [16], information matrices [17], or other dynamic features [18], [19].

Among possible fusion techniques, the Kalman filter (KF)-based estimator remain most popular due to simplicity, optimality, and low computational burden [20]–[23]. However, it is known that the optimality does not always go along with the robustness and fault tolerance required by the WSN operation conditions. The problem is that optimal estimators require all information about an object and its measurement, which is typically unavailable in practice [24], [25].

Another issue is that measurements via WSNs are often accompanied with missing data due to external factors such as electromagnetic interference, unstable links, faulty behavior of the sensors, etc. [26]. Therefore, an algorithm must be capable of providing accurate estimation under temporarily lost data as shown in many papers. For example, the state error covariance is bounded in [27] by introducing a critical value for the data arrival rate. In [20], the issue was solved by combining node estimates at the previous and current time points. The problem complicates by the fact that the KF estimate is affected by model errors and inappropriate

The associate editor coordinating the review of this manuscript and approving it for publication was Ghufran Ahmed.

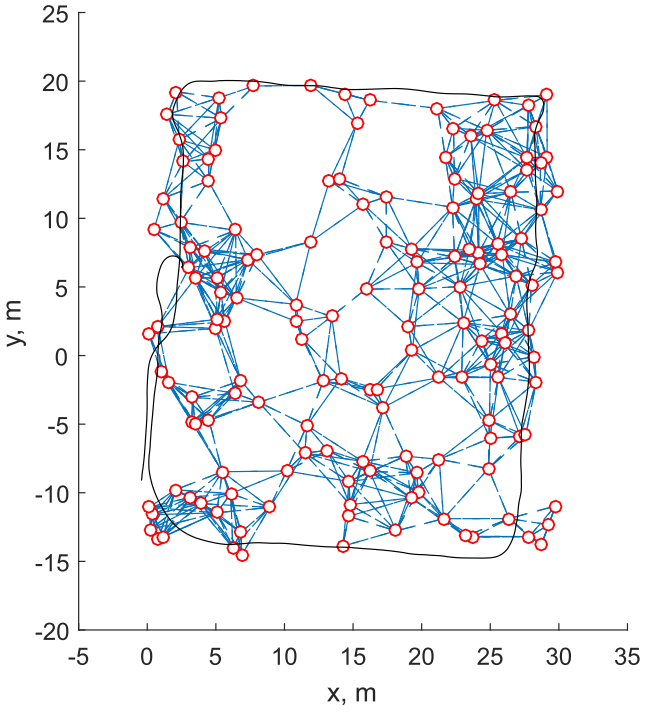

FIGURE 1. An example of a WSN composed of 150 nodes with 687 links (dotted). The WSN covers the moving object trajectory (solid) with the number of the links limited with the nodes ranges.

noise behavior. Moreover, errors caused by missed data propagate along the entire estimation process.

As an alternative to the KF, there was developed a more robust approach employing properties of finite impulse response (FIR) filtering [25], [28]. Based upon this approach, the authors of [21] proposed a fusion technique using the optimal unbiased FIR (OUFIR) filter, which is more robust than the KF. In [11], [29], different types of consensus were taken into account using advantages of the unbiased FIR (UFIR) filter, which performs better than the KF under the real world operation conditions. Nevertheless, still no UFIR solution was addressed to designers of distributed WSNs with missing data that motivates our present work.

In this paper, we design a distributed UFIR (dUFIR) filter for object tracking via WSNs with consensus on estimates under measurements with missing data. We show that the dUFIR filter outperforms the distributed KF (dKF) in terms of accuracy and robustness. The rest of the paper is organized as follows. Section II discusses the model and formulates the problem. In Section III, a design of the tracking predictive dUFIR filter is given both in the batch and fast iterative forms along with the predictive dKF. Simulations are provided in Section IV and conclusions are drawn in Section VI.

II. MOVING OBJECT MODEL IN DISTRIBUTED WSNs AND PROBLEM FORMULATION

In the state-space formulation, dynamics of a moving object can be described in discrete time index k and K-state space for a general scenario of distributed WSNs with missing data using the following equations,

$$x_k = F_k x_{k-1} + B_k w_k, \tag{1}$$
$$\bar{y}_k^{(i)} = H_k^{(i)} F_k x_{k-1}, \tag{2}$$
$$y_k^{(i)} = \gamma_k (H_k^{(i)} x_k + v_k^{(i)}) + (1-\gamma_k)\bar{y}_k^{(i)}, \tag{3}$$
$$y_k = H_k x_x + v_k, \tag{4}$$

where $x_k \in \mathbb{R}^K$, $F_k \in \mathbb{R}^{K\times K}$, and $B_k \in \mathbb{R}^{K\times L}$. Measurements of $\mathcal{Q}_k$ are provided at each k with $J \triangleq J_k$ nodes. The ith, $i \in [1, J]$, node measures x_k by $y_k^{(i)} \in \mathbb{R}^p$, $p \leqslant K$, with $H_k^{(i)} \in \mathbb{R}^{p\times K}$ and each node has J inclusive neighbors. Local data $y_k^{(i)}$ are united in the observation vector $y_k = [\, y_k^{(i)^T} \ \dots \ y_k^{(J)^T} \,]^T \in \mathbb{R}^{Jp}$ with $H_k = [\, H_k^{(i)^T} \ \dots \ H_k^{(J)^T} \,]^T \in \mathbb{R}^{Jp\times K}$. Noise vectors $w_k \in \mathbb{R}^L$ and $v_k = [\, v_k^{(1)^T} \ \dots \ v_k^{(n)^T} \,]^T \in \mathbb{R}^{Jp}$ are zero mean, not obligatorily white Gaussian, uncorrelated, and with the covariances $Q_k = E\{w_k w_k^T\} \in \mathbb{R}^{L\times L}$, $R_k = \text{diag}[\, R_k^{(1)^T} \ \dots \ R_k^{(n)^T} \,]^T \in \mathbb{R}^{Jp\times Jp}$, and $R_k^{(i)} = E\{v_k^{(i)} v_k^{(i)^T}\}$.

A binary variable γ_k serves as an indicator of whether data exist ($\gamma_k = 1$) or not ($\gamma_k = 0$). When $\gamma_k = 0$, the predicted measurement $\bar{y}_k^{(i)}$ (2) is used by substituting x_{k-1} with the estimate. In the following section, we will present the design of a batch dUFIR filter with optimal consensus on estimates that minimizes the mean square error (MSE). We will also show that the dUFIR filter designed outperforms the dKF in terms of the localization robustness for measurements with missing data.

III. TRACKING FILTERING ALGORITHMS WITH CONSENSUS ON ESTIMATES

If to regard a WSN as an undirected graph $\mathcal{G} = (\mathcal{V}, \mathcal{E})$ where each vertex $v^{(i)} \in \mathcal{V}$ is a node and each link is an edge of set $\mathcal{E}$, for $i \in \mathcal{I} = \{1, \dots, n\}$ and $n = |\mathcal{V}|$. As stated in [15], nodes $v^{(i)}$ and $v^{(j)}$ reach an agreement if and only if states are related as $x^{(i)} = x^{(j)}$, $\{i, j\} \in \mathcal{I}$, $i \neq j$. Under such a condition, the network reaches a consensus with the common value of all nodes called the *group decision value*.

For the nodes to reach an agreement, a consensus protocol must minimize the total disagreement in the network by minimizing the Laplacian potential of the graph $\Psi = \frac{1}{2} x^T L x$, where L is the Laplacian matrix. A known linear distributed protocol for minimizing the total disagreement is

$$u^{(i)} = \sum_j^J (x^{(j)} - x^{(i)}). \tag{5}$$

In what follows, we achieve the consensus of estimates by implementing (5) in two different algorithms: one based on the dKF and the other one on the dUFIR filter. The dKF requires that every first order neighbor shares the estimate of a local KF and that the ith node implements another KF with the consensus protocol (5) to reach the group decision value. In the dUFIR, the consensus on estimates is achieved using data only of the inclusive neighbors in (5). Details of the designed algorithms follow next.

A. DISTRIBUTED KF ALGORITHM

The dKF with consensus on estimates was proposed in [16]. An idea behind this solution is to provide individual estimates in each node using the KF and then use another KF to fuse them. A pseudo code of the dKF algorithm augmented with a prediction option for temporarily lost data is shown as Algorithm 1.

Algorithm 1 Iterative dKF Algorithm

Data: $P_0^{(i)}, Q_k, R_k^{(j)}, \bar{x}_k^{(j)}, y_k^{(j)}, \bar{x}_0^{(i)} = x_0$
Result: $\hat{x}_k^{(i)}$

1 **begin**
2 **for** $k = 0 : \infty$ **do**
3 **if** $\gamma_k = 0$ **then**
4 $y_k^{(j)} = H_k^{(j)} F_k \hat{x}_{k-1}^{(j)}$;
5 **end if**
6 $z_k^{(j)} = H_k^{(j)^T} R_k^{(j)^{-1}} y_k^{(j)}$;
7 $s_k^{(i)} = \sum_{j\in J} z_k^{(j)}$;
8 $Z_k^{(j)} = H_k^{(j)^T} R_k^{(j)^{-1}} H_k^{(j)}$;
9 $S_k^{(i)} = \sum_{j\in J} Z_k^{(j)}$;
10 $M_k^{(i)} = (P_k^{(i)^{-1}} + S_k^{(i)})^{-1}$;
11 $\hat{x}_k^{(i)} = \bar{x}_k^{(i)} + M_k^{(i)}(s_k^{(i)} - S_k^{(i)}\bar{x}_k^{(i)}) + \epsilon M_k^{(i)} \sum_{j\in J}(\bar{x}_k^{(j)} - \bar{x}_k^{(i)})$;
12 $P_k^{(i)} \leftarrow F_k M_k^{(i)} F_k^T + B_k Q_k B_k^T$;
13 $\bar{x}_k^{(i)} \leftarrow F_k \hat{x}_k^{(i)}$;
14 **end for**
15 **end**

Its specific is that, in order to reach a consensus on estimate when some data are temporarily lost, an unavailable measurement at k is predicted (lines 3–5) via the available estimate $\bar{x}_k^{(j)}$ at $k-1$ in each of the nodes. Because all data are needed from all of the neighbors, the dKF algorithm must ensure that the prediction is available from all of the neighbors.

B. DISTRIBUTED UFIR FILTER ALGORITHM

Unlike the dKF, which operates from one point to another using optimal recursions, the UFIR filter operates on finite horizons of N points and therefore exists in the convolution-based batch form and fast iterative form using recursions. Below, we show both these forms.

1) EXTENDED STATE-SPACE MODEL

To apply FIR filtering, model (1)–(4) for $\gamma_k = 1$ must be extended on a horizon $[m, k]$ of N points, from $m = k-N+1$ to k, as in the following [28],

$$X_{m,k} = A_{m,k} x_m + D_{m,k} W_{m,k}, \tag{6}$$
$$Y_{m,k} = C_{m,k} x_m + M_{m,k} W_{m,k} + V_{m,k}, \tag{7}$$
$$Y_{m,k}^{(i)} = C_{m,k}^{(i)} x_m + M_{m,k}^{(i)} W_{m,k} + V_{m,k}^{(i)}, \tag{8}$$

where

$$X_{m,k} = \begin{bmatrix} x_m^T & x_{m+1}^T & \dots & x_k^T \end{bmatrix}^T,$$
$$Y_{m,k} = \begin{bmatrix} y_m^T & y_{m+1}^T & \dots & y_k^T \end{bmatrix}^T,$$
$$W_{m,k} = \begin{bmatrix} w_m^T & w_{m+1}^T & \dots & w_k^T \end{bmatrix}^T,$$
$$V_{m,k} = \begin{bmatrix} v_m^T & v_{m+1}^T & \dots & v_k^T \end{bmatrix}^T,$$
$$Y_{m,k}^{(i)} = \begin{bmatrix} y_m^{(i)^T} & y_{m+1}^{(i)^T} & \dots & y_k^{(i)^T} \end{bmatrix}^T,$$
$$V_{m,k}^{(i)} = \begin{bmatrix} v_m^{(i)^T} & v_{m+1}^{(i)^T} & \dots & v_k^{(i)^T} \end{bmatrix}^T,$$

and the extended matrices are

$$A_{m,k} = [\, I \; F_{m+1}^T \dots (\mathcal{F}_{k-1}^{m+1})^T \,]^T, \tag{9}$$

$$D_{m,k} = \begin{bmatrix} B_m & 0 & \dots & 0 & 0 \\ F_{m+1}B_m & B_{m+1} & \dots & 0 & 0 \\ \vdots & \vdots & \ddots & \vdots & \vdots \\ \mathcal{F}_{k-1}^{m+1} B_m & \mathcal{F}_{k-1}^{m+2} B_{m+1} & \dots & B_{k-1} & 0 \\ \mathcal{F}_k^{m+1} B_m & \mathcal{F}_k^{m+2} B_{m+1} & \dots & F_k B_{k-1} & Bk \end{bmatrix}, \tag{10}$$

$C_{m,k} = \bar{C}_{m,k} A_{m,k}$, $M_{m,k} = \bar{C}_{m,k} D_{m,k}$, $C_{m,k}^{(i)} = \bar{C}_{m,k}^{(i)} A_{m,k}$, $M_{m,k}^{(i)} = \bar{C}_{m,k}^{(i)} D_{m,k}$, where

$$\bar{C}_{m,k} = \mathrm{diag}(H_m \; H_{m+1} \; \dots \; H_k), \tag{11}$$
$$\bar{C}_{m,k}^{(i)} = \mathrm{diag}(H_m^{(i)} \; H_{m+1}^{(i)} \; \dots \; H_k^{(i)}), \tag{12}$$
$$\mathcal{F}_r^g = \begin{cases} F_r F_{r-1} \dots F_g, & g < r+1 \\ I, & g = r+1 \\ 0, & g > r+1. \end{cases} \tag{13}$$

Based on model (6)–(8), the batch dUFIR filter can be designed as shown below.

2) BATCH DUFIR FILTER

The FIR estimate for model (6)–(8) can be obtained as

$$\hat{x}_k = \Theta_{m,k} Y_{m,k}, \tag{14}$$

where $\Theta_{m,k}$ is the FIR filter gain (impulse response) obeying some cost function [28]. To obtain the dUFIR filter, let us suppose that the ith node provides a local estimate over data (8) as $\hat{x}_k^{(i)}$. Then, referring to [16], the consensus between the local estimates can be found if to introduce a vector $\Sigma_k = \sum_j^J [\hat{x}_k^{(j)} - \hat{x}_k^{(i)}]$, combine it with (14), and write the estimate as

$$\hat{x}_k^{\mathrm{c}} = \Theta_{m,k} Y_{m,k} + \lambda_k \Sigma_k, \tag{15}$$

where λ_k is a scaling factor to be optimized in the MSE sense.

For the dUFIR filter, gain $\Theta_{m,k}$ must be found to obey the unbiased condition

$$E\{\hat{x}_k^{\mathrm{c}}\} = E\{\hat{x}_k^{(i)}\} = E\{x_k\}$$

and the dUFIR estimate will thus be robust against errors in the noise statistics and initial values [28].

Referring to (6)–(8), estimate (15) can be rewritten as

$$\hat{x}_k^{\mathrm{c}} = \Theta_{m,k} Y_{m,k} + J\lambda_k \Theta_{m,k} Y_{m,k} - J\lambda_k \Theta_{m,k}^{(i)} Y_{m,k}^{(i)}, \quad (16)$$

where gains $\Theta_{m,k}$ and $\Theta_{m,k}^{(i)}$, which obey the unbiasedness condition [28], are represented with

$$\begin{aligned} \Theta_{m,k} &= (I + J\lambda_k)(\mathcal{H}_{m,k}^T \mathcal{H}_{m,k})^{-1} \mathcal{H}_{m,k}^T, && (17a)\\ &= (I + J\lambda_k) G_k \mathcal{H}_{m,k}^T, && (17b)\\ \Theta_{m,k}^{(i)} &= (\mathcal{H}_{m,k}^{(i)^T} \mathcal{H}_{m,k}^{(i)})^{-1} \mathcal{H}_{m,k}^{(i)^T}, && (18a)\\ &= G_k^{(i)} \mathcal{H}_{m,k}^{(i)^T}, && (18b) \end{aligned}$$

where $G_k^{(i)} = (\mathcal{H}_{m,k}^{(i)^T} \mathcal{H}_{m,k}^{(i)})^{-1}$ is the generalized noise power gain (GNPG) [30], and

$$\mathcal{H}_{m,k} = \begin{bmatrix} H_m (\mathcal{F}_k^{m+1})^{-1} \\ H_{m+1} (\mathcal{F}_k^{m+2})^{-1} \\ \vdots \\ H_{k-1} F_k^{-1} \\ H_k \end{bmatrix}, \quad (19)$$

$$\mathcal{H}_{m,k}^{(i)} = \begin{bmatrix} H_m^{(i)} (\mathcal{F}_k^{m+1})^{-1} \\ H_{m+1}^{(i)} (\mathcal{F}_k^{m+2})^{-1} \\ \vdots \\ H_{k-1}^{(i)} F_k^{-1} \\ H_k^{(i)} \end{bmatrix}. \quad (20)$$

As can be seen, information required to compute $\Theta_{m,k}$ and $\Theta_{m,k}^{(i)^T}$ is entirely provided by the K-state space model, which can be preloaded on the nodes. Thus, only measurement data will be sent by the node, unlike the dKF case implying that each node must wait for the individual estimate of its neighbors. This reduces the number of exchange messages and improves battery life.

The optimal scaling factor λ_k^{opt} can be obtained by solving the optimization problem

$$\lambda_k^{\mathrm{opt}} = \arg\min_{\lambda_k} \{\mathrm{tr}\, P_k(\lambda_k)\},$$

where $P_k = E\{\varepsilon_k \varepsilon_k^T\}$ is the error covariance matrix and $\varepsilon_k = x_k - \hat{x}_k^{\mathrm{c}}$ is the estimation error. By solving the optimization problem, λ_k^{opt} can be shown to be (see Appendix A)

$$\begin{aligned} \lambda_k^{\mathrm{opt}} = -\frac{1}{J} &(\tilde{\Theta}_{m,k} \bar{R}_{m,k} \tilde{\Theta}_{m,k}^T - G_k G_k^{(i)^{-1}} \Theta_{m,k}^{(i)} \\ &\times \bar{R}_{m,k}^{(i)} \Theta_{m,k}^{(i)^T})(\tilde{\Theta}_{m,k} \bar{R}_{m,k} \tilde{\Theta}_{m,k}^T - 2 G_k G_k^{(i)^{-1}} \\ &\times \Theta_{m,k}^{(i)} \bar{R}_{m,k}^{(i)} \Theta_{m,k}^{(i)^T} + \Theta_{m,k}^{(i)} \bar{R}_{m,k}^{(i)} \Theta_{m,k}^{(i)^T})^{-1}. \quad (21) \end{aligned}$$

where $\tilde{\Theta}_{m,k} = G_k \mathcal{H}_{m,k}^T$ and

$$\begin{aligned} \bar{R}_{m,k} &= E\{v_{m,k} v_{m,k}^T\} = \mathrm{diag}(R_m \dots R_k), && (22)\\ \bar{R}_{m,k}^{(i)} &= E\{v_{m,k}^{(i)} v_{m,k}^{(i)^T}\} = \mathrm{diag}(R_m^{(i)} \dots R_k^{(i)}). && (23) \end{aligned}$$

Although (21) is affected by measurement noise, it remains invariant to system noise, that definitely results in higher robustness of the dUFIR filter.

A flaw of the batch dUFIR filter is that the implementation of (15) with (21) on a high-density WSN and large horizons N require a large-dimension matrix operation, which is not suitable for smart sensors. A fast computation can be provided using an iterative algorithm, which we will consider next.

3) ITERATIVE dUFIR FILTERING ALGORITHM

An iterative form of the estimate $\hat{x}_k^{\mathrm{c}}$ can be obtained if to represent $\hat{x}_k^{\mathrm{c}}$ with a sum of a centralized estimate $\hat{x}_k$ defined by (14) and a local estimate $\hat{x}_k^{(i)} = \Theta_{m,k}^{(i)} Y_{m,k}^{(i)}$. That allows writing (16) as

$$\hat{x}_k^{\mathrm{c}} = (I + J\lambda_k)\hat{x}_k - J\lambda_k \hat{x}_k^{(i)}, \quad (24)$$

and, following [11], [28], find recursions. Namely, for $\hat{x}_k$, one can employ from [28]

$$\begin{aligned} G_l &= [H_l^T H_l + (F_l G_{l-1} F_l^T)^{-1}]^{-1}, && (25)\\ \hat{x}_l^- &= F_l \hat{x}_{l-1}, && (26)\\ \hat{x}_l &= \hat{x}_l^- + G_l H_l^T (y_l - H_l \hat{x}_l^-), && (27) \end{aligned}$$

and

$$\begin{aligned} G_l^{(i)} &= [H_l^{(i)^T} H_l^{(i)} + (F_l G_{l-1}^{(i)} F_l^T)^{-1}]^{-1}, && (28)\\ \hat{x}_l^{(i)^-} &= F_l \hat{x}_{l-1}^{(i)}, && (29)\\ \hat{x}_l^{(i)} &= \hat{x}_l^{(i)^-} + G_l^{(i)} H_l^{(i)^T} (y_l^{(i)} - H_l^{(i)} \hat{x}_l^{(i)^-}), && (30) \end{aligned}$$

where l is an iterative variable starting at $s = k - N + K$, where K is the number of the states, and ending when $l = k$.

Iterations using (25)–(27) can be initialized with $G_{l-1} = G_s$ and $\hat{x}_{l-1} = \hat{x}_s$ in short batch forms of

$$\begin{aligned} G_s &= (\mathcal{H}_{m,s}^T \mathcal{H}_{m,s})^{-1}, && (31)\\ \hat{x}_s &= G_s \mathcal{H}_{m,s}^T Y_{m,s}. && (32) \end{aligned}$$

Following the same strategy, iterations (28)–(30) for $\hat{x}_k^{(i)}$ can be initialized with

$$\begin{aligned} G_s^{(i)} &= (\mathcal{H}_{m,s}^{(i)^T} \mathcal{H}_{m,s}^{(i)})^{-1}, && (33)\\ \hat{x}_s^{(i)} &= G_s^{(i)} \mathcal{H}_{m,s}^{(i)^T} Y_{m,s}^{(i)}. && (34) \end{aligned}$$

Finally, fast computation of factor λ_k^{opt} can be provided if to represent (21) as

$$\begin{aligned} \lambda_k^{\mathrm{opt}} = -\frac{1}{J} &(\alpha_k - G_k G_k^{(i)^{-1}} \beta_k) \\ &\times (\alpha_k - 2 G_k G_k^{(i)^{-1}} \beta_k + \beta_k)^{-1}, \quad (35) \end{aligned}$$

where $\alpha_k = \tilde{\Theta}_{m,k} \bar{R}_{m,k} \tilde{\Theta}_{m,k}^T$ and $\beta_k = \Theta_{m,k}^{(i)} \bar{R}_{m,k}^{(i)} \Theta_{m,k}^{(i)^T}$, and use the recursions (see Appendix B and Appendix C)

$$\begin{aligned} \alpha_k &= G_k (H_k^T R_k H_k + F_k^{-T} G_{k-1}^{-1} \alpha_{k-1} G_{k-1}^{-1} F_k^{-1}) G_k && (36)\\ \beta_k &= G_k^{(i)} (H_k^{(i)^T} R_k^{(i)} H_k^{(i)} + F_k^{-T} G_{k-1}^{(i)^{-1}} \beta_{k-1} G_{k-1}^{(i)^{-1}} F_k^{-1}) G_k^{(i)}, && (37) \end{aligned}$$

which initial values α_{k-1} and β_{k-1} can be computed in short batch forms as

$$\alpha_s = G_s \mathcal{H}_{m,s}^T \bar{R}_{m,s} \mathcal{H}_{m,s} G_s^T, \tag{38}$$

$$\beta_s = G_s^{(i)} \mathcal{H}_{m,s}^{(i)^T} \bar{R}_{m,s}^{(i)} \mathcal{H}_{m,s}^{(i)} G_s^{(i)^T}. \tag{39}$$

A pseudo code of the predictive iterative dUFIR algorithm with consensus on estimates designed for measurements with temporary missing data is listed as Algorithm 2. Given a

Algorithm 2 Iterative dUFIR Filtering Algorithm

Data: $y_k, R_k^{(i)}, R_k, N$
Result: $\hat{x}_k$
begin
  for $k = N-1 : \infty$ **do**
    $m = k - N + 1, \quad s = m + K - 1;$
    $G_s = (\mathcal{H}_{m,s}^T \mathcal{H}_{m,s})^{-1};$
    $G_s^{(i)} = (\mathcal{H}_{m,s}^{(i)^T} \mathcal{H}_{m,s}^{(i)})^{-1};$
    if $\gamma_k = 0$ **then**
      $y_k^{(j)} = H_k^{(j)} F_k \hat{x}_{k-1}^{(j)};$
    end if
    $\tilde{x}_s = G_s \mathcal{H}_{m,s}^T Y_{m,s};$
    $\tilde{x}_s^{(i)} = G_s^{(i)} \mathcal{H}_{m,s}^{(i)^T} Y_{m,s}^{(i)};$
    $\alpha_s = G_s \mathcal{H}_{m,s}^T \bar{R}_{m,s} \mathcal{H}_{m,s} G_s^T;$
    $\beta_s = G_s^{(i)} \mathcal{H}_{m,s}^{(i)^T} \bar{R}_{m,s}^{(i)} \mathcal{H}_{m,s}^{(i)} G_s^{(i)^T};$
    for $l = s+1 : k$ **do**
      $\hat{x}_l^- = F_l \hat{x}_{l-1};$
      $\hat{x}_l^{(i)^-} = F_l \hat{x}_{l-1}^{(i)};$
      $G_l = [H_l^T H_l + (F_l G_{l-1} F_l^T)^{-1}]^{-1};$
      $G_l^{(i)} = [H_l^{(i)^T} H_l^{(i)} + (F_l G_{l-1}^{(i)} F_l^T)^{-1}]^{-1};$
      $\hat{x}_l = \hat{x}_l^- + G_l H_l^T (y_l - H_l \hat{x}_l^-);$
      $\hat{x}_l^{(i)} = \hat{x}_l^{(i)^-} + G_l^{(i)} H_l^{(i)^T} (y_l^{(i)} - H_l^{(i)} \hat{x}_l^{(i)^-});$
      $\alpha_l =$
      $G_l (H_l^T R_l H_l + F_l^{-T} G_{l-1}^{-1} \alpha_{l-1} G_{l-1}^{-1} F_l^{-1}) G_l;$
      $\beta_l = G_l^{(i)} (H_l^{(i)^T} R_l^{(i)} H_l^{(i)} +$
      $F_l^{-T} G_{l-1}^{(i)^{-1}} \beta_{l-1} G_{l-1}^{(i)^{-1}} F_l^{-1}) G_l^{(i)};$
    end for
    $\lambda_k =$
    $-\frac{1}{J}(\alpha_k - G_k G_k^{(i)^{-1}} \beta_k)(\alpha_k - 2\, G_k G_k^{(i)^{-1}} \beta_k + \beta_k)$
    $\hat{x}_k^c = (I + J\lambda_k)\tilde{x}_k - J\lambda_k \tilde{x}_k^{(i)};$
  end for
end
† First data $y_0, y_1, ..., y_{N-1}$ must be available.

horizon of N points, Algorithm 2 starts computing the initial values at $s = m+K-1$ and then updates the results beginning at $s+1$ until the iterative variable l reaches k. It then computes the optimal consensus factor λ_k and finishes with the output estimate $\hat{x}_k^c$.

In what follows, we will test Algorithm 2 along with the dKF Algorithm 1 originally proposed in [16]. A numerical example will be given for tracking of a circularly traveling and rapidly maneuvering object. Experimental verification will be provided for robot localization with measured ground truth.

TABLE 1. Nodes sorted by the number of available links with neighbors.

	Number of links						
	2	3	4	5	6	7	9
Node	8,12,16	1	4,5,6,13,14,15	18	2,3,17	7,11	9,10

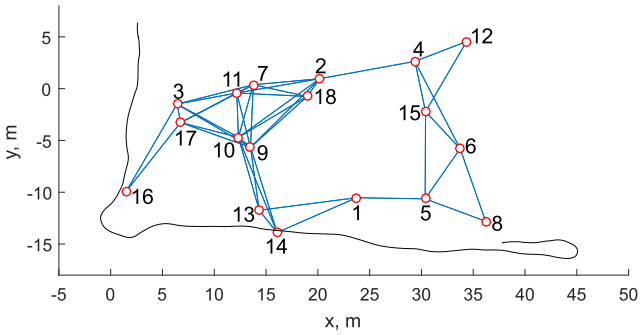

FIGURE 2. WSN over a ground truth trajectory available from the MagPIE project dataset [31].

IV. MANEUVERING OBJECT TRACKING WITH MISSING DATA

To conduct this experiment, we employ the ground truth trajectory available for free from the MagPIE project dataset [31]. We consider a random WSN composed of 18 nodes whose connections are sketched in Fig. 2 and listed in Table 1. Every node is capable of measuring the object Cartesian coordinates x and y of the mobile robot location. Measurements were simulated by adding white Gaussian noise to the ground truth data in each of the sensors. Noise was generated to have the variance $\sigma_v^{(i)} = 0.25 + \phi$, where ϕ is uniformly distributed as $\phi = U(0.5, -0.5)$.

Supposing that some data can be lost in communication channels, we remove some data obeying the binomial distribution with the probability of $P = 0.9$ as shown in Fig 3. Note that each node has different sets of lost data.

The moving object dynamics are given in state space by

$$A = \begin{bmatrix} 1 & \tau & 0 & 0 \\ 0 & 1 & 0 & 0 \\ 0 & 0 & 1 & \tau \\ 0 & 0 & 0 & 1 \end{bmatrix}, \quad H^{(i)} = \begin{bmatrix} 1 & 0 & 0 & 0 \\ 0 & 0 & 1 & 0 \end{bmatrix},$$

$$B = \begin{bmatrix} \tau/2 & 0 \\ 1 & 0 \\ 0 & \tau/2 \\ 0 & 1 \end{bmatrix}, \quad Q = \begin{bmatrix} \sigma_w^2 & 0 \\ 0 & \sigma_w^2 \end{bmatrix},$$

where $\sigma_w = 0.76$ m/s. For dUFIR, the optimal horizon N_{opt} was found at a test stage to be 53 in average.

As stated by (21), the optimal factor λ_k^{opt} depends on the appropriate knowledge of the noise statistics. To analyze the robustness of the algorithms, we let $Q_k \leftarrow (0.1)^2 Q_k$ and

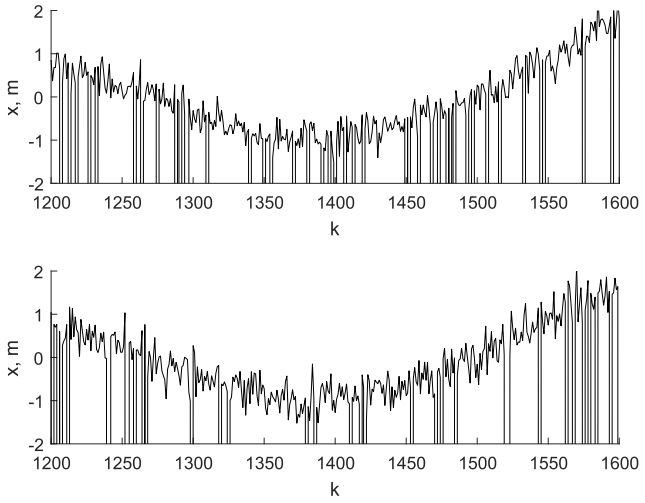

FIGURE 3. Measurements along coordinate x with missing data for: a) node 10 and b) node 12.

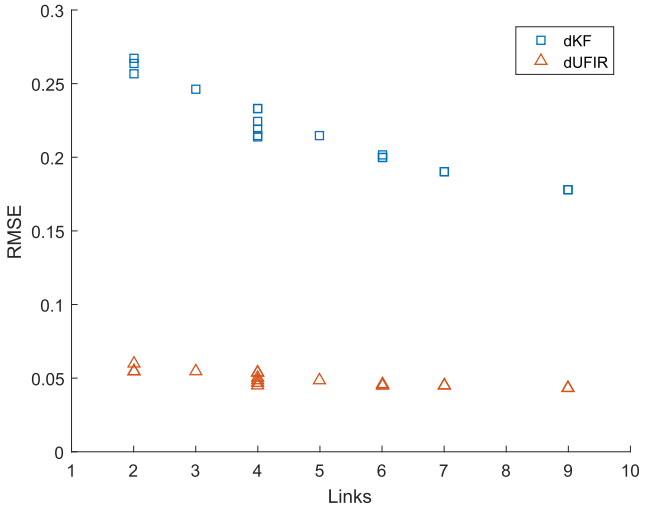

FIGURE 4. RMSE produced by each node of the WSN.

$R_k^{(i)} \leftarrow q^{(i)^2} R_k^{(i)}$ where $q^{(i)} = U(1,2)$, meaning that each sensor has different errors in the noise statistics.

As has been shown in [11], the estimation error decreases by an increase in the number of the links. As follows from Fig. 4 sketching the RMSE produced by each node, this also holds true for the consensus on estimates. In fact, despite the effect of noise uncertainties in (20), the dUFIR filter errors range in Fig. 4 much lower than by the dKF. Also, the dUFIR filter demonstrates lesser variations in the individual RMSEs. The latter means that the dUFIR filter provided a better consensus than the dKF. Effect of errors in the noise covariance on the dKF estimate is easily seen in Fig. 5. Under large uncertainties in noise, the dKF fails to produce low estimation errors, which is more evident for a small number of the neighbors (Fig. 5 a). But even under the larger number of the neighbors, the dUFIR filter still outperforms the dKF (Fig. 5 b).

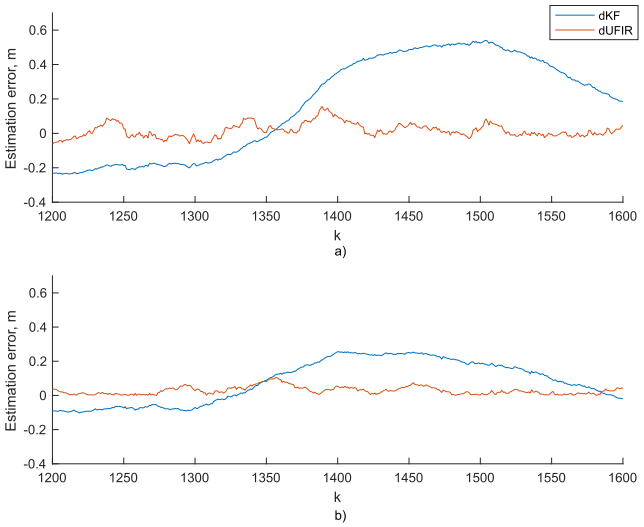

FIGURE 5. Estimation error produced by the dUFIR filter and dKF under error in the noise covariances: a) node 12 with 2 links and b) node 10 with 9 links.

V. VEHICLE LOCALIZATION OVER WSN WITH MISSING DATA AND TIME-VARYING MODEL NOISE

In this section we consider a WSN with 30 nodes, which covers a trajectory of an unmanned ground vehicle (UGV) (robot). The trajectory shown in Fig. 6 is available for free use from the MagPIE dataset [31]. Each node is equipped with a time-of-flight (ToF) ranging sensor VL53L0X and a MEMS gyro ADXRS649. The measuring distance $\rho_k^{(i)}$ of the ith ToF sensor is limited with 2 m and an accuracy of $\Delta\rho_k^{(i)} = 4.8$ cm. The MEMS gyro has an angular resolution of $\Delta\phi_k^{(i)} = 0.47°$ for a measured angle $\phi_k^{(i)}$. The communication range of each node is limited with 5 m.

When an UGV enters in the node range, a distance and an angle are measured as $\rho_k^{(i)} = \bar{\rho}_k^{(i)} + \Delta\rho_k^{(i)}$ and $\phi_k^{(i)} = \bar{\phi}_k^{(i)} + \Delta\phi_k^{(i)}$, respectively, with a sampling time of $T = 0.01\,s$, where $\bar{\rho}_k^{(i)}$ and $\bar{\phi}_k^{(i)}$ are average values and $\Delta\rho_k^{(i)}$ and $\Delta\phi_k^{(i)}$ are white Gaussian and uncorrelated with the standard deviations of $\sigma_{\rho k} = |\Delta\rho_k^{(i)}|/3$ and $\sigma_{\phi k} = |\Delta\phi_k^{(i)}|/3$. The UGV altitude is ignored in our experiment. To avoid nonlinearities inherent to polar coordinates, we represent the UGV Cartesian coordinates as $x_k^{(i)} = \rho_k^{(i)} \cos\phi_k^{(i)} = \bar{x}_k^{(i)} + \Delta x_k^{(i)}$ and $y_k^{(i)} = \rho_k^{(i)} \sin\phi_k^{(i)} = \bar{y}_k^{(i)} + \Delta y_k^{(i)}$ and approximate with

$$\begin{aligned} x_k^{(i)} &= (\bar{\rho}_k^{(i)} + \Delta\rho_k^{(i)})\cos(\bar{\phi}_k^{(i)} + \Delta\phi_k^{(i)}), \\ &\cong \bar{\rho}_k^{(i)} \cos\bar{\phi}_k^{(i)} + \Delta\rho_k^{(i)} \cos\bar{\phi}_k^{(i)} - \Delta\phi_k^{(i)} \bar{\rho}_k^{(i)} \sin\bar{\phi}_k^{(i)}, \quad (40) \\ y_k^{(i)} &= (\bar{\rho}_k^{(i)} + \Delta\rho_k^{(i)})\sin(\bar{\phi}_k^{(i)} + \Delta\phi_k^{(i)}), \\ &\cong \bar{\rho}_k^{(i)} \sin\bar{\phi}_k^{(i)} + \Delta\rho_k^{(i)} \sin\bar{\phi}_k^{(i)} + \Delta\phi_k^{(i)} \bar{\rho}_k^{(i)} \cos\bar{\phi}_k^{(i)}, \quad (41) \end{aligned}$$

where $\bar{x}_k^{(i)} = \bar{\rho}_k^{(i)} \cos\bar{\phi}_k^{(i)}$, $\bar{y}_k^{(i)} = \bar{\rho}_k^{(i)} \sin\bar{\phi}_k^{(i)}$, $\Delta x_k^{(i)} = \Delta\rho_k^{(i)} \cos\bar{\phi}_k^{(i)} - \Delta\phi_k^{(i)} \bar{\rho}_k^{(i)} \sin\bar{\phi}_k^{(i)}$, and $\Delta y_k^{(i)} = \Delta\rho_k^{(i)} \sin\bar{\phi}_k^{(i)} + \Delta\phi_k^{(i)} \bar{\rho}_k^{(i)} \cos\bar{\phi}_k^{(i)}$.

For this model, we define the measurement noise variances as $\sigma_{xk}^{(i)^2} = E\{\Delta x_k^{(i)^2}\}$ and $\sigma_{yk}^2 = E\{\Delta y_k^{(i)^2}\}$, ignore products of

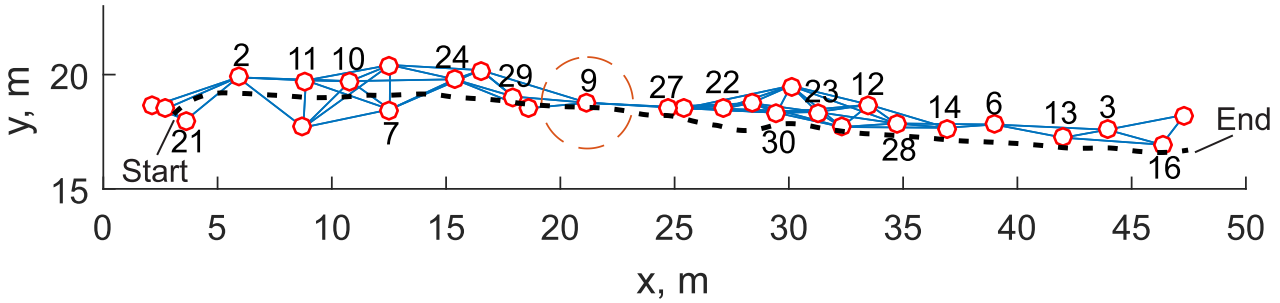

FIGURE 6. A WSN covering the UGV trajectory available from the MagPIE dataset [31]. The labeled nodes are used in the reconstruction of the trajectory. The dashed circle exhibits the 2 m range of a ToF sensor.

small and uncorrelated values $\Delta\rho_k^{(i)}$ and $\Delta\phi_k^{(i)}$, provide

$$\sigma_{\mathrm{x}k}^{(i)} = \sigma_{\rho k}^2 \cos^2\bar{\phi}_k + \sigma_{\phi k}^2 \bar{\rho}_k^2 \sin^2\bar{\phi}_k = \frac{(\Delta\rho_k^{(i)})^2}{9}\cos^2\bar{\phi}_k + \frac{(\Delta\phi_k^{(i)})^2}{9}\bar{\rho}_k^2 \sin^2\bar{\phi}_k \quad (42)$$

$$\sigma_{\mathrm{y}k}^{(i)} = \sigma_{\rho k}^2 \sin^2\bar{\phi}_k + \sigma_{\phi k}^2 \bar{\rho}_k^2 \cos^2\bar{\phi}_k = \frac{(\Delta\rho_k^{(i)})^2}{9}\sin^2\bar{\phi}_k + \frac{(\Delta\phi_k^{(i)})^2}{9}\bar{\rho}_k^2 \cos^2\bar{\phi}_k, \quad (43)$$

and describe the time-varying measurement noise covariance matrix as

$$R_k^{(i)} = \begin{bmatrix} \sigma_{\mathrm{x}k}^{(i)} & 0 \\ 0 & \sigma_{\mathrm{y}k}^{(i)} \end{bmatrix}.$$

The UGV dynamics and the covariance Q are exactly the same as in the previous section. The nodes available for the UGV at each k due to limited range are listed in Table 2.

Estimation of the UGV trajectory via the WSN has been obtained by combining estimates by the nodes labeled in Fig. 6 and bolded in Table 2, which communicate with nearest neighbors (not bolded in Table 2). To test the algorithms for different available information about noise, we consider several possible scenarios of filter tuning. In each of the cases, we evaluate effects of deviations from $\Delta\rho_k = 4.8$ cm and $\Delta\phi_k = 0.47°$ specified in the maximum sense on the filter performance via (42) and (43).

In the first and second scenarios, measurement data are simulated assuming that the normally distributed zero mean noise has the same variances of $(\Delta\rho_k^{(i)})^2 = 4.8^2$ and $(\Delta\phi_k^{(i)})^2 = 0.47^2$ for $i = \{1, \ldots, 30\}$ in all sensors. In the remaining four scenarios, we generate different measurement data supposing that the normally distributed zero noise has different variances in each sensor. In this case, the variances are uniformly distributed with $(\Delta\rho_k^{(i)})^2 \sim \mathrm{U}(3.6^2, 4.8^2)$ and $(\Delta\phi_k^{(i)})^2 \sim \mathrm{U}(0.1173^2, 0.47^2)$ for $i = \{1, \ldots, 30\}$. In the first four scenarios, the dUFIR filter is tuned to $N_{\mathrm{opt}} = 13$. In the first five scenarios, the dKF undergoes the effect of errors in the noise statistics caused by $Q \leftarrow p^2\, Q_k$ with $p = 4$. The scenarios are the following:

1) *SC-1:* Set $\Delta\rho_k^{(i)} = 4.8$ cm and $\Delta\phi_k^{(i)} = 0.47°$.
2) *SC-2:* Reduce $\Delta\rho_k^{(i)}$ and $\Delta\phi_k^{(i)}$ by the factor of 3 as an error of the known sensor noise.
3) *SC-3:* Distribute sensor errors uniformly as $\Delta\rho_k^{(i)} \sim \mathrm{U}(3.6, 4.8)$, in cm, and $\Delta\phi_k^{(i)} \sim \mathrm{U}(0.1173°, 0.47°)$, but set $\Delta\rho_k^{(i)} = 4.8$ cm and $\Delta\phi_k^{(i)} = 0.47°$.

TABLE 2. Nodes available in different time intervals of index k.

Time index k	Node index	Time index k	Node index
1 - 89	17,20,**21**	1208 -1287	**22**,26,27
90 - 90	20,**21**	1287 -1290	**22**,26
91 - 123	**2**,20,21	1290 -1324	5,**22**,26
124 - 165	**2**,21	1324 -1343	5,**22**
166 - 277	**2**	1343 -1404	5,22,**30**
278 - 300	2,**11**	1404 -1417	5,**30**
301 - 324	2,4,**11**	1417 -1425	5,25,**30**
325 - 397	4,**11**	1425 -1467	5,**23**,25,30
398 - 464	4,**10**,11	1467 -1476	**23**,25,30
465 - 481	**10**,11	1476 -1514	19,**23**,25,30
482 - 486	**7**,10,11	1514 -1534	19,**23**,30
487 - 502	**7**,10	1534 -1559	19,**23**
503 - 586	**7**,10,15	1559 -1602	**12**,19,23
587 - 624	**7**,15	1602 -1619	12,19,23,**28**
625 - 652	7,15,**24**	1619 -1681	12,19,**28**
653 - 668	7,**24**	1681 -1712	12,**28**
669 - 690	**24**	1712 -1714	12,**14**,28
691 - 739	18,**24**	1714 -1792	**14**,28
740 - 772	18,24,**29**	1792 -1817	**14**
773 - 797	1,18,24,**29**	1817 -1892	**6**,14
798 - 836	1,18,**29**	1892 -1946	**6**
837 - 898	1,**29**	1946 -1980	6,**13**
899 - 931	1,**9**,29	1980 -2037	**13**
932 - 962	1,**9**	2037 -2117	**3**,13
963 - 1066	**9**	2117 -2135	**3**
1067 - 1087	9,**27**	2135 -2200	3,**16**
1088 - 1105	**27**	2200 -2228	**16**
1106 - 1207	26,**27**	2228 -2300	8,**16**

TABLE 3. RMSEs produced by dKF and dUFIR filter.

Scenario	dKF	dUFIR
SC1	0.0081	**0.0077**
SC2	0.0097	**0.0077**
SC3	0.0071	**0.0070**
SC4	0.0084	**0.0070**
SC5	0.0073	**0.0069**
SC6	0.0091	**0.0069**

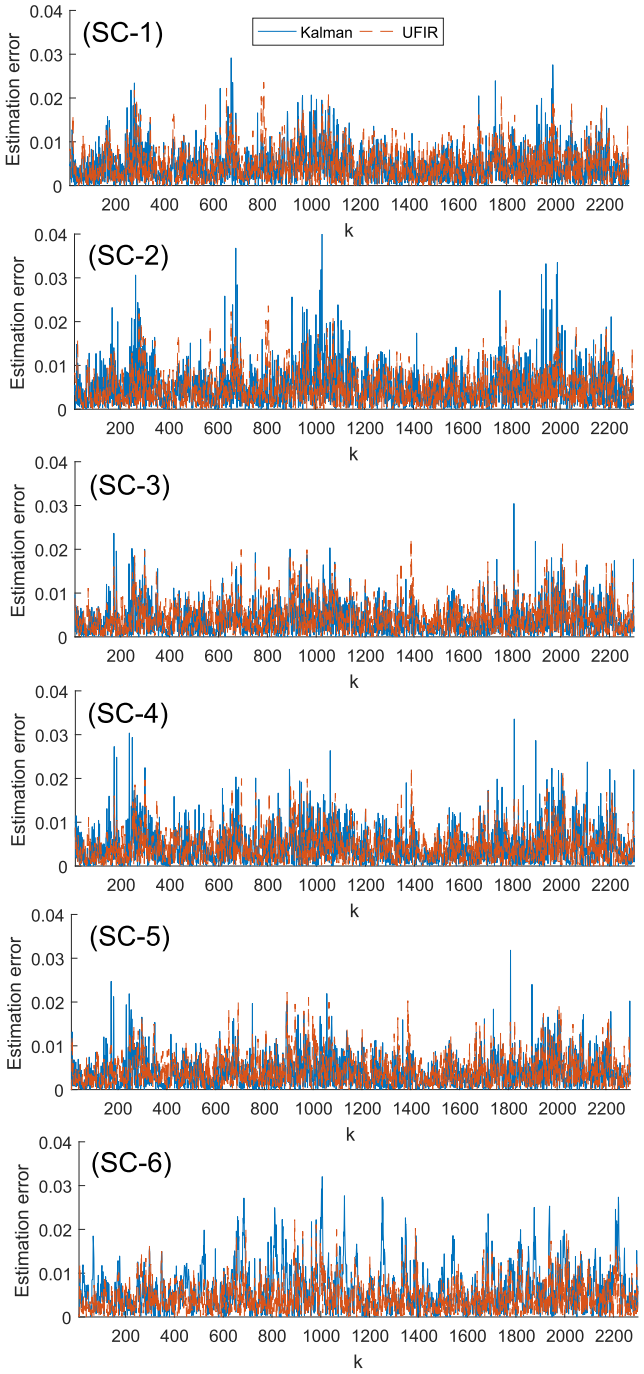

FIGURE 7. Absolute estimation errors along the coordinate x produced by the dKF and dUFIR filter for six scenarios, (SC-1)–(SC-6).

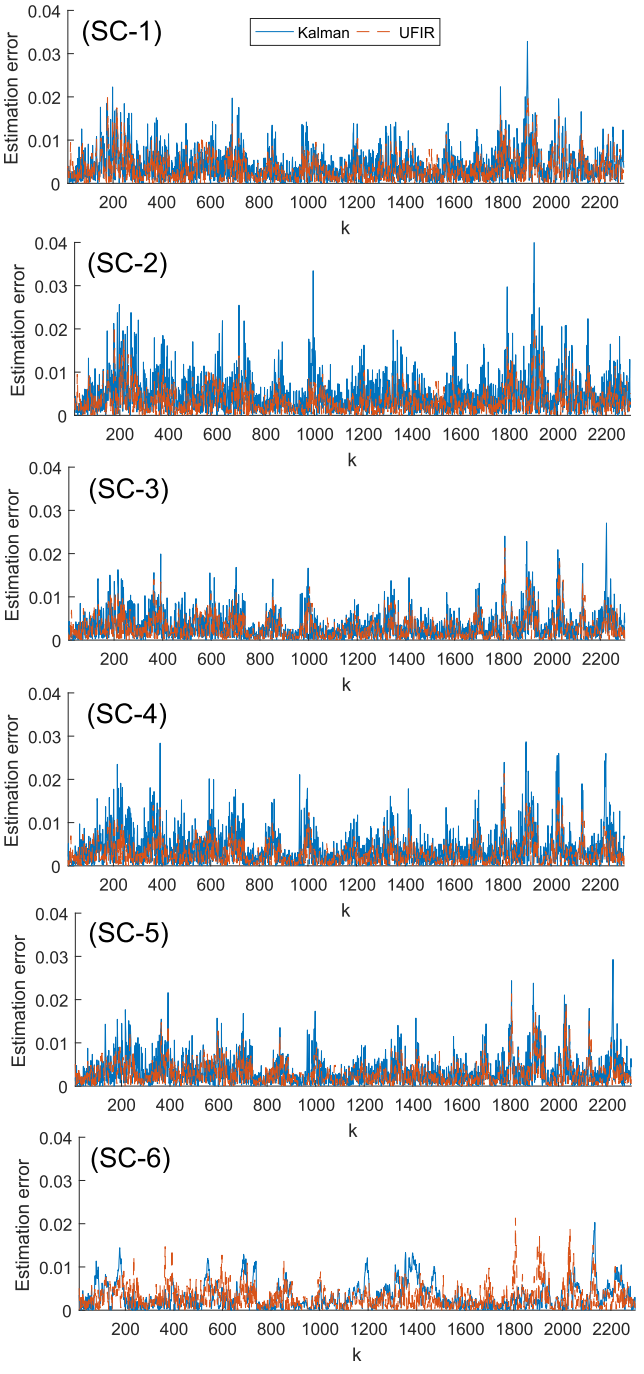

FIGURE 8. Absolute estimation errors along the coordinate y produced by the dKF and dUFIR filter for six scenarios, (SC-1)–(SC-6).

4) *SC-4:* as in SC-3, distribute errors uniformly as $\Delta\rho_k^{(i)} \sim \mathrm{U}(3.6, 4.8)$, in cm, and $\Delta\phi_k^{(i)} \sim \mathrm{U}(0.1173°, 0.47°)$ and set $\Delta\rho_k^{(i)} = \frac{4.8}{3}$ cm and $\Delta\phi_k^{(i)} = \frac{0.47}{3}°$.
5) *SC-5:* Set $\Delta\rho_k^{(i)}$ randomly taken from $\mathrm{U}(3.6, 4.8)$, in cm, and $\Delta\phi_k^{(i)}$ from $\mathrm{U}(0.1173°, 0.47°)$. Set $N_{\text{opt}}^{(i)}$ individually to each sensor.
6) *SC-6:* Consider SC-5 for $Q \leftarrow p^2\, Q_k$ with $p = 0.1$.

In terms of the absolute estimation errors, the results are sketched in Fig. 7 along the coordinate x and in Fig. 8 along y and one can easily trace the differences. The first point to notice is that the dUFIR filter in general outperforms the dKF in each of the above scenarios. To support this inference, the RMSEs computed by the root square of the sum of the MSEs along coordinates x and y are listed in Table 3, where the minimum values are bolded.

Of a particular interest is the case of SC-6 illustrated in Fig. 8. While the dUFIR estimate remains here unaltered by errors in Q, the dKF reduces the estimation random errors in specific time intervals, such as $1500 \leq k \leq 2000$. However,

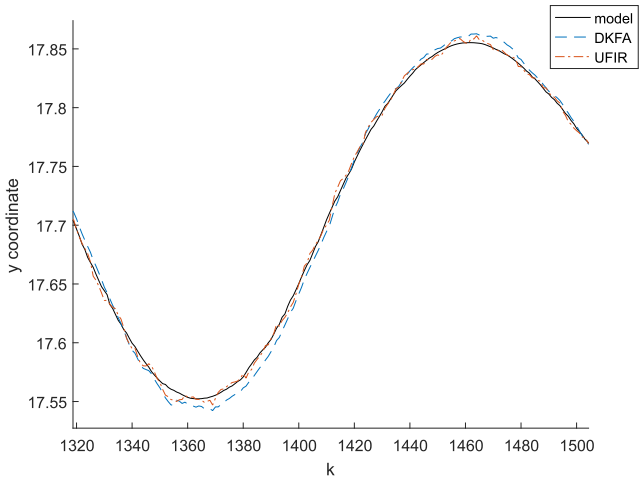

FIGURE 9. Estimates provided by the dKF and dUFIR filter along the coordinate y for scenario SC-6.

in $1300 \leq k \leq 1500$ the bias error produced by dKF grows considerably (Fig. 9) that speaks in favor of higher robustness of the dUFIR filter.

VI. CONCLUSION

In this paper, the problem of object tracking over distributed WSNs with consensus on estimates and missing data has been solved by designing and using the dUFIR filter. Better performance of the dUFIR filter-based localization system has been proven with respect to known ground truth through simulations for measurements with missing data and referring to real sensor specifications. Extensive experimental investigations have shown that the dUFIR filter produces smaller errors than the dKF under uncertainties in the noise statistics and model errors. It was also verified that the dUFIR filter allows reaching a better consensus in estimates than the dKF in terms of errors in individual estimates. Another noticeable advantage of the dUFIR filter, which was observed in simulations, is that it requires a smaller number of the nodes to achieve the same performance as in the dKF. Referring to the above advantages of the dUFIR filter, we are now designing a hybrid estimator of a moving object trajectory to reach a consensus on both the estimates and measurements.

APPENDIX A
CONSENSUS FACTOR λ_k^{opt}

Consider the error covariance $P_k = E\{\varepsilon_k \varepsilon_k^T\}$ as function of λ_k, to be

$$\begin{aligned} P_k &= (\bar{D}_{m,k} - \tilde{\Theta}_{m,k} M_{m,k}) Q_{m,k} (\bar{D}_{m,k} - \tilde{\Theta}_{m,k} M_{m,k})^T \\ &+ J\lambda_k (\tilde{\Theta}_{m,k} \bar{R}_{m,k} \tilde{\Theta}_{m,k}^T - \Theta_{m,k}^{(i)} \tilde{R}^{(i)^T} \tilde{\Theta}_{m,k}^T) \\ &+ J[\lambda_k (\tilde{\Theta}_{m,k} \bar{R}_{m,k} \tilde{\Theta}_{m,k}^T - \Theta_{m,k}^{(i)} \tilde{R}^{(i)^T} \tilde{\Theta}_{m,k}^T)]^T \\ &+ J^2 \lambda_k (\tilde{\Theta}_{m,k} \bar{R}_{m,k} \tilde{\Theta}_{m,k}^T - \tilde{\Theta}_{m,k} \tilde{R}_{m,k}^{(i)} \Theta_{m,k}^{(i)^T}) \lambda_k^T \\ &+ J^2 \lambda_k (\Theta_{m,k}^{(i)} \tilde{R}^{(i)^T} \tilde{\Theta}_{m,k}^T + \Theta_{m,k}^{(i)} \bar{R}_{m,k}^{(i)} \Theta_{m,k}^{(i)^T}) \lambda_k^T, \end{aligned} \tag{A.1}$$

where $\tilde{\Theta}_{m,k} = G_k \mathcal{H}_{m,k}^T$ and

$$\begin{aligned} \bar{R}_{m,k} &= E\{v_{m,k} v_{m,k}^T\} = \text{diag}(R_m \dots R_k), \\ \bar{R}_{m,k}^{(i)} &= E\{v_{m,k}^{(i)} v_{m,k}^{(i)^T}\} = \text{diag}(R_m^{(i)} \dots R_k^{(i)}), \\ \tilde{R}_{m,k}^{(i)} &= E\{v_{m,k} v_{m,k}^{(i)^T}\} = \text{diag}(\tilde{R}_m^{(i)} \dots \tilde{R}_k^{(i)}). \end{aligned}$$

We next apply the derivative with respect to λ_k to the trace of (A.1) by using the identities $\frac{\partial}{\partial X} \text{tr}(X^T B X) = BX + B^T X$, and $\frac{\partial}{\partial X} \text{tr}(XA) = A^T$. Putting the derivative to zero yields

$$\begin{aligned} \lambda_k^{\text{opt}} &= -\frac{1}{J} (\tilde{\Theta}_{m,k} \bar{R}_{m,k} \tilde{\Theta}_{m,k}^T - \tilde{\Theta}_{m,k} \tilde{R}_{m,k}^{(i)} \Theta_{m,k}^{(i)^T}) \\ &\times (\tilde{\Theta}_{m,k} \bar{R}_{m,k} \tilde{\Theta}_{m,k}^T - \tilde{\Theta}_{m,k} \tilde{R}_{m,k}^{(i)} \Theta_{m,k}^{(i)^T} \\ &- (\tilde{\Theta}_{m,k} \tilde{R}_{m,k}^{(i)} \Theta_{m,k}^{(i)^T})^T + \Theta_{m,k}^{(i)} \bar{R}_{m,k}^{(i)} \Theta_{m,k}^{(i)^T}), \end{aligned} \tag{A.2}$$

and with the identities

$$\begin{aligned} \tilde{\Theta}_{m,k} \tilde{R}_{m,k}^{(i)} \Theta_{m,k}^{(i)^T} &= (\tilde{\Theta}_{m,k} \tilde{R}_{m,k}^{(i)} \Theta_{m,k}^{(i)^T})^T, \\ \tilde{\Theta}_{m,k} \tilde{R}_{m,k}^{(i)} \Theta_{m,k}^{(i)^T} &= G_k G_k^{(i)^{-1}} \Theta_{m,k}^{(i)} \bar{R}_{m,k}^{(i)} \Theta_{m,k}^{(i)^T}, \end{aligned} \tag{A.3}$$

we obtain the final form of (21).

APPENDIX B
RECURSION FOR α_l

Consider $\alpha_k = \tilde{\Theta}_{m,k} \bar{R}_{m,k} \tilde{\Theta}_{m,k}^T$ in (35) and rewrite it as

$$\alpha_k = G_k \mathcal{H}_{m,k} \bar{R}_{m,k} \mathcal{H}_{m,k}^T G_k. \tag{B.1}$$

Represent the product $\mathcal{H}_{m,k} \bar{R}_{m,k} \mathcal{H}_{m,k}^T$ by the sum of

$$\begin{aligned} \mathcal{H}_{m,k} \bar{R}_{m,k} \mathcal{H}_{m,k}^T &= \sum_{l=0}^{N-1} (\mathcal{F}_k^{m+1+l})^{-T} \\ &\times H_{m+l}^T R_{m+l} H_{m+l} (\mathcal{F}_k^{m+1+l})^{-1} \end{aligned} \tag{B.2}$$

$$\begin{aligned} &= H_k^T R_k H_k + F_k^{-T} \Bigg[\sum_{l=0}^{N-2} (\mathcal{F}_{k-1}^{m+1+l})^{-T} \\ &\times H_{m+l}^T R_{m+l} H_{m+l} (\mathcal{F}_{k-1}^{m+1+l})^{-1} \Bigg] F_k^{-1} \end{aligned} \tag{B.3}$$

$$\begin{aligned} &= H_k^T R_k H_k \\ &+ F_k^{-T} \mathcal{H}_{m,k-1} \bar{R}_{m,k-1} \mathcal{H}_{m,k-1}^T F_k^{-1}. \end{aligned} \tag{B.4}$$

Referring to $\alpha_{k-1} = G_{k-1} \mathcal{H}_{m,k-1} \bar{R}_{m,k-1} \mathcal{H}_{m,k-1}^T G_{k-1}$, find

$$\mathcal{H}_{m,k-1} \bar{R}_{m,k-1} \mathcal{H}_{m,k-1}^T = G_{k-1}^{-1} \alpha_{k-1} G_{k-1}^{-1}. \tag{B.5}$$

Finally, combine (B.1), (B.4), and (B.5) and end up with the recursion (36) for α_k.

APPENDIX C
RECURSION FOR β_k

Rewrite $\beta_k = \Theta_{m,k}^{(i)} \bar{R}_{m,k}^{(i)} \Theta_{m,k}^{(i)^T}$ in (35) as

$$\beta_k = G_k^{(i)} \mathcal{H}_{m,k}^{(i)} \bar{R}_{m,k}^{(i)} \mathcal{H}_{m,k}^{(i)^T} G_k^{(i)}, \tag{C.1}$$

represent by the sum, and transform as

$$\mathcal{H}_{m,k}^{(i)}\bar{R}_{m,k}^{(i)}\mathcal{H}_{m,k}^{(i)^T} = \sum_{l=0}^{N-1}(\mathcal{F}_k^{m+1+l})^{-T} \times H_{m+l}^{(i)^T}R_{m+l}^{(i)}H_{m+l}^{(i)}(\mathcal{F}_k^{m+1+l})^{-1} \tag{C.2}$$

$$= H_k^{(i)^T}R_k^{(i)}H_k^{(i)} + F_k^{-T}\left[\sum_{l=0}^{N-2}(\mathcal{F}_{k-1}^{m+1+l})^{-T} \times H_{m+l}^{(i)^T}R_{m+l}^{(i)}H_{m+l}^{(i)}(\mathcal{F}_{k-1}^{m+1+l})^{-1}\right]F_k^{-1} \tag{C.3}$$

$$= H_k^{(i)^T}R_k^{(i)}H_k^{(i)} + F_k^{-T}\mathcal{H}_{m,k-1}^{(i)}\bar{R}_{m,k-1}^{(i)}\mathcal{H}_{m,k-1}^{(i)^T}F_k^{-1}. \tag{C.4}$$

From $G_{k-1}^{(i)}\mathcal{H}_{m,k-1}^{(i)}\bar{R}_{m,k-1}^{(i)}\mathcal{H}_{m,k-1}^{(i)^T}G_{k-1}^{(i)}$ find

$$\mathcal{H}_{m,k-1}^{(i)}\bar{R}_{m,k-1}^{(i)}\mathcal{H}_{m,k-1}^{(i)^T} = G_{k-1}^{(i)^{-1}}\beta_{k-1}G_{k-1}^{(i)^{-1}}, \tag{C.5}$$

combine (C.1), (C.4), and (C.5), and arrive at the recursion (37) for β_k.

REFERENCES

[1] J. Lin, W. Xiao, F. L. Lewis, and L. Xie, "Energy-efficient distributed adaptive multisensor scheduling for target tracking in wireless sensor networks," *IEEE Trans. Instrum. Meas.*, vol. 58, no. 6, pp. 1886–1896, Jun. 2009.

[2] C. Liang, F. Wen, and Z. Wang, "Trust-based distributed Kalman filtering for target tracking under malicious cyber attacks," *Inf. Fusion*, vol. 46, pp. 44–50, Mar. 2019.

[3] J. Yick, B. Mukherjee, and D. Ghosal, "Wireless sensor network survey," *Comput. Netw.*, vol. 52, no. 12, pp. 2292–2330, Aug. 2008.

[4] I. F. Akyildiz, W. Su, Y. Sankarasubramaniam, and E. Cayirci, "Wireless sensor networks: A survey," *Comput. Netw.*, vol. 38, no. 4, pp. 393–422, 2002.

[5] M. S. Mahmoud and Y. Xia, *Networked Filtering and Fusion in Wireless Sensor Networks*. Boca Raton, FL, USA: CRC Press, 2014.

[6] C. Chen, S. Zhu, X. Guan, and X. Shen, *Wireless Sensor Networks*. New York, NY, USA: Springer, 2014.

[7] B. S. Rao and H. F. Durrant-Whyte, "Fully decentralised algorithm for multisensor Kalman filtering," *IEE Proc. D-Control Theory Appl.*, vol. 138, no. 5, pp. 413–420, 1991.

[8] D. Wang, L. Lin, and L. Xu, "A study of subdividing hexagon-clustered WSN for power saving: Analysis and simulation," *Ad Hoc Netw.*, vol. 9, no. 7, pp. 1302–1311, Sep. 2011.

[9] M. Kohvakka, J. Suhonen, M. Kuorilehto, V. Kaseva, M. Hännikäinen, and T. D. Hämäläinen, "Energy-efficient neighbor discovery protocol for mobile wireless sensor networks," *Ad Hoc Netw.*, vol. 7, no. 1, pp. 24–41, Jan. 2009.

[10] J. Roselin, P. Latha, and S. Benitta, "Maximizing the wireless sensor networks lifetime through energy efficient connected coverage," *Ad Hoc Netw.*, vol. 62, no. 4, pp. 1–10, Jul. 2017.

[11] M. Vazquez-Olguin, Y. S. Shmaliy, and O. G. Ibarra-Manzano, "Distributed unbiased FIR filtering with average consensus on measurements for WSNs," *IEEE Trans. Ind. Informat.*, vol. 13, no. 3, pp. 1440–1447, Jun. 2017.

[12] H. Dong, Z. Wang, and H. Gao, "Distributed filtering for a class of time-varying systems over sensor networks with quantization errors and successive packet dropouts," *IEEE Trans. Signal Process.*, vol. 60, no. 6, pp. 3164–3173, Jun. 2012.

[13] I. D. Schizas, A. Ribeiro, and G. B. Giannakis, "Consensus in ad hoc WSNs with noisy links—Part I: Distributed estimation of deterministic signals," *IEEE Trans. Signal Process.*, vol. 56, no. 1, pp. 350–364, Jan. 2008.

[14] E. Nurellari, D. McLernon, and M. Ghogho, "Distributed two-step quantized fusion rules via consensus algorithm for distributed detection in wireless sensor networks," *IEEE Trans. Signal Inf. Process. Netw.*, vol. 2, no. 3, pp. 321–335, Sep. 2016.

[15] R. Olfati-Saber, "Distributed Kalman filter with embedded consensus filters," in *Proc. 44th IEEE Conf. Decis. Control*, Dec. 2005, pp. 8179–8184.

[16] R. Olfati-Saber, "Distributed Kalman filtering for sensor networks," in *Proc. 46th IEEE Conf. Decis. Control*, Dec. 2007, pp. 5492–5498.

[17] W. Li, Z. Wang, G. Wei, L. Ma, J. Hu, and D. Ding, "A survey on multisensor fusion and consensus filtering for sensor networks," *Discrete Dyn. Nature Soc.*, vol. 2015, Sep. 2015, Art. no. 683701.

[18] N. Rahbari-Asr and M.-Y. Chow, "Cooperative distributed demand management for community charging of PHEV/PEVs based on KKT conditions and consensus networks," *IEEE Trans. Ind. Informat.*, vol. 10, no. 3, pp. 1907–1916, Aug. 2014.

[19] W. Yu, L. Zhou, X. Yu, J. Lü, and R. Lu, "Consensus in multi-agent systems with second-order dynamics and sampled data," *IEEE Trans. Ind. Informat.*, vol. 9, no. 4, pp. 2137–2146, Nov. 2013.

[20] X. Bai, Z. Wang, L. Zou, and F. E. Alsaadi, "Collaborative fusion estimation over wireless sensor networks for monitoring CO_2 concentration in a greenhouse," *Inf. Fusion*, vol. 42, pp. 119–126, Jul. 2018.

[21] S. Zhao, Y. S. Shmaliy, and C. K. Ahn, "Bias-constrained optimal fusion filtering for decentralized WSN with correlated noise sources," *IEEE Trans. Signal Inf. Process. Netw.*, vol. 4, no. 4, pp. 727–735, Dec. 2018.

[22] S. R. Jondhale and R. S. Deshpande, "Kalman filtering framework-based real time target tracking in wireless sensor networks using generalized regression neural networks," *IEEE Sensors J.*, vol. 19, no. 1, pp. 224–233, Jan. 2018.

[23] H. Qian, P. Fu, B. Li, J. Liu, and X. Yuan, "A novel loss recovery and tracking scheme for maneuvering target in hybrid WSNs," *Sensors*, vol. 18, no. 2, p. 341, Jan. 2018.

[24] J. J. Pomarico-Franquiz and Y. S. Shmaliy, "Accurate self-localization in RFID tag information grids using FIR filtering," *IEEE Trans. Ind. Informat.*, vol. 10, no. 2, pp. 1317–1326, May 2014.

[25] Y. S. Shmaliy, S. Khan, and S. Zhao, "Ultimate iterative UFIR filtering algorithm," *Measurement*, vol. 92, pp. 236–242, Oct. 2016.

[26] L. Pan, H. Gao, H. Gao, and Y. Liu, "A spatial correlation based adaptive missing data estimation algorithm in wireless sensor networks," *Int. J. Wireless Inf. Netw.*, vol. 21, no. 4, pp. 280–289, Oct. 2014.

[27] B. Sinopoli, L. Schenato, M. Franceschetti, K. Poolla, M. I. Jordan, and S. S. Sastry, "Kalman filtering with intermittent observations," *IEEE Trans. Autom. Control*, vol. 49, no. 9, pp. 1453–1464, Sep. 2004.

[28] Y. S. Shmaliy, S. Zhao, and C. K. Ahn, "Unbiased finite impluse response filtering: An iterative alternative to Kalman filtering ignoring noise and initial conditions," *IEEE Control Syst. Mag.*, vol. 37, no. 5, pp. 70–89, Oct. 2017.

[29] M. Vazquez-Olguin, Y. S. Shmaliy, and O. Ibarra-Manzano, "Developing UFIR filtering with consensus on estimates for distributed wireless sensor networks," *WSEAS Trans. Circuits Syst.*, vol. 17, pp. 30–37, 2018.

[30] Y. S. Shmaliy and O. Ibarra-Manzano, "Noise power gain for discrete-time FIR estimators," *IEEE Signal Process. Lett.*, vol. 18, no. 4, pp. 207–210, Apr. 2011.

[31] D. Hanley, A. B. Faustino, S. D. Zelman, D. A. Degenhardt, and T. Bretl, "MagPIE: A dataset for indoor positioning with magnetic anomalies," in *Proc. IEEE Int. Conf. Indoor Positioning Indoor Navigat. (IPIN)*, Sep. 2017, pp. 1–8.

MIGUEL VAZQUEZ-OLGUIN (M'16) was born in Mexico, in 1982. He received the B.S. degree in electronics and communications from the Universidad Iberoamericana de León, León, Mexico, in 2005, and the M.S. degree in electronics and communications from the Center for Scientific Research and Higher Education of Ensenada, Ensenada, Mexico, in 2009. He is currently pursuing the Ph.D. degree with the Universidad de Guanajuato, Salamanca, Mexico. His current research interests include consensus filtering, wireless sensor networks, and optimal estimation.

YURIY S. SHMALIY (M'96–SM'00–F'11) received the B.S., M.S., and Ph.D. degrees from the Kharkiv Aviation Institute, Ukraine, in 1974, 1976, and 1982, respectively, all in electrical engineering. He received the D.Sc. degree from the Kharkiv Railroad Institute, in 1992.

He served as a Full Professor, in 1986. From1985 to 1999, he was with Kharkiv Military University. In 1992, he founded the Scientific Center Sichron, where he was the Director, in 2002. Since 1999, he has been with the Universidad de Guanajuato, Mexico, where he was the Head of the Department of Electronics Engineering, from 2012 to 2015. From 2015 to 2016, he was a Visiting Researcher with the City, University of London, and in 2015 and 2017–2019, he has been with Telecom SudParis. He has 447 journal and conference papers and holds 81 patents. His books are *Continuous-Time Signals* (Springer, 2006), *Continuous-Time Systems* (Springer, 2007), and *GPS-Based Optimal FIR Filtering of Clock Models* (New York: Nova Science Publishers, 2009). He also edited a book *Probability: Interpretation, Theory and Applications* (New York: Nova Science Publishers, 2012) and contributed to several books with invited chapters. He was rewarded a title Honorary Radio Engineer of the USSR, in 1991. His current interests include optimal estimation, statistical signal processing, and stochastic system theory. He was listed in the Outstanding People of the 20th Century, Cambridge, U.K., in 1999, and has received the Royal Academy of Engineering Newton Research Collaboration Program Award, in 2015. He is currently an Associate Editor and an Editorial Board Member in several journals. He was invited many times to give tutorial, seminar, and plenary lectures.

OSCAR IBARRA-MANZANO (M'00) was born in Mexico, in 1968. He received the B.S. degree in communications and electronics and the M.E. degree in electrical engineering from the Universidad de Guanajuato, Salamanca, in 1990 and 1993, respectively, and the Ph.D. degree in electrical engineering from the National Institute for Astrophysics Optics and Electronics, Puebla, Mexico, in 1999. In 1991, he joined the Universidad de Guanajuato, where he has been a full-time Professor and the Chair of the Electronics Engineering Department, since 2000, and served as the Dean for the Mechanical, Electrical and Electronics Engineering School, from 2003 to 2012.

JORGE MUNOZ-MINJARES (M'14) was born in Zacatecas, Mexico, in 1987. He received the B.S. degree in communications and electronics engineering from the Universidad Autonoma de Zacatecas, in 2010, and the M.S. and Ph.D. degrees in electrical engineering from DICIS, Universidad de Guanajuato, in 2012 and 2018, respectively. He is currently an Assistant Professor with the Universidad Tecnologica de Salamanca. His research interests include digital signal and image processing, optimal filtering, and probability and statistics.

CARLOS LASTRE-DOMINGUEZ (M'17) was born in Sincé, Colombia, in 1987. He received the B.S. degree from the Universidad de Pamplona, Colombia, in 2011, and the M.I. degree from the Universidad Industrial de Santander, Santander, Colombia, in 2016. He is currently pursuing the Ph.D. degree in electrical engineering with the Universidad de Guanajuato. His scientific research interests include machine learning, digital signal processing, and optimum filter applied to biomedical signals. He has also participated in various congresses on these topics.